Production cross-sections of protactinium and thorium isotopes produced in fragmentation of ^{238}U at 1 A GeV

J. Kurcewicz [a,*], Z. Liu [b], M. Pfützner [a], P.J. Woods [b], C. Mazzocchi [c], K.-H. Schmidt [c], A. Kelić [c], F. Attallah [c], E. Badura [c], C.N. Davids [d], T. Davinson [b], J. Döring [c], H. Geissel [c], M. Górska [c], R. Grzywacz [e], M. Hellström [c], Z. Janas [a], M. Karny [a], A. Korgul [a], I. Mukha [c], C. Plettner [c], A. Robinson [b], E. Roeckl [c], K. Rykaczewski [e], K. Schmidt [f], D. Seweryniak [d], K. Sümmerer [c], H. Weick [c]

[a] *Institute of Experimental Physics, Warsaw University, ul. Hoża 69, PL-00-681 Warsaw, Poland*

[b] *School of Physics, University of Edinburgh, James Clerk Maxwell Building, The King's Buildings, Mayfield Road, Edinburgh EH9 3JZ, UK*

[c] *Gesellschaft für Schwerionenforschung mbH, Planckstr. 1, D-64291 Darmstadt, Germany*

[d] *Physics Division, Argonne National Laboratory, 9700 S. Cass Avenue, Argonne, IL 60439, USA*

[e] *Physics Division, Oak Ridge National Laboratory, 1 Bethel Valley Road, Oak Ridge, TN 37831, USA*

[f] *University of Applied Sciences Coburg, Friedrich-Streib-Str. 2, D-96450 Coburg, Germany*

Abstract

The production cross-sections of proton-rich protactinium and thorium isotopes have been investigated for the fragmentation of 1 A GeV ^{238}U in a beryllium target at the SIS/FRS facility at GSI Darmstadt. The experimental results are compared with the predictions of an abrasion-ablation model of nuclear fragmentation yielding good overall agreement. Weak evidence for first observation of new isotopes ^{208}Th and ^{211}Pa is presented.

Key words: Fragmentation reactions, proton-rich isotopes, suburanium isotopes
PACS: 25.70.Mn, 29.30.Aj

1 Introduction

Projectile fragmentation reactions have been proven to be very powerful for the study of exotic nuclei, including proton-rich ones up to $A \simeq 100$ [1]. Compared with fusion-evaporation reactions, projectile fragmentation reactions, especially at high energies, have the advantages of allowing the use of large target thicknesses and very short flight-time. In principle, projectile fragmentation of ^{238}U at relativistic energy can thus be applied, as an alternative to fusion-evaporation reactions, to the production and decay spectroscopy of heavier very proton-rich isotopes. However, previous studies have shown that the production cross-sections of neutron-deficient near-projectile fragments from ^{208}Pb and ^{238}U induced reactions are reduced compared to reactions induced by lighter projectiles, due to the influence of fission [2]. Moreover, the wide ionic-charge distribution of heavy projectile-like fragments means that the yields for a given charge state selected by a magnetic spectrometer is reduced. Therefore, the investigations of production cross-sections of projectile-fragmentation products in the suburanium region, representing a significant challenge as such, are important for testing model predictions and planning future decay-spectroscopic experiments.

This paper provides experimentally determined production cross-sections of light protactinium and thorium isotopes from the reaction of ^{238}U (1 A GeV) on beryllium. The measured data are compared with the experimental results of the reaction of ^{238}U (1 A GeV) on hydrogen [3] and with predictions of the abrasion-ablation model of nuclear fragmentation. The results related to α-spectroscopy of suburanium isotopes obtained in this experiment have been presented in Ref. [4].

2 Experiment

The experiment was performed at the SIS synchrotron of GSI Darmstadt, which delivered a 1 A GeV ^{238}U beam in spills lasting 6 s with a repetition period of 10-18 s. The beam impinged on a 1023 mg/cm^2 thick beryllium target placed at the entrance to the Projectile Fragment Separator (FRS) [5]. The primary beam intensity was of the order of 10^8 ions/spill. The ^{238}U intensity was recorded by a secondary-electron transmission monitor [6]. The reaction products were separated by the FRS operated in the standard achromatic mode. The FRS, combining two stages of magnetic selection and an energy loss in a degrader, allows a full identification of reaction products with respect

* Corresponding author. Tel: +48-22-8231896; Fax: +48-22-8237647
Email address: jan.kurcewicz@fuw.edu.pl (J. Kurcewicz).

to their nuclear charge Z and mass A. After the first magnetic selection, reaction products are slowed down in a thick aluminium degrader located at the intermediate focal plane. A second magnetic selection is applied to the ions leaving the degrader. To decrease the abundance of not-fully stripped ions, a niobium foil stripper was placed both behind the target and the degrader.

The time-of-flight measurement was performed between two plastic scintillator detectors, one located in the intermediate focal plane and the other one at the final focus. These scintillators provided also the horizontal position of fragments passing the respective FRS positions. The time-of-flight for the isotopes of interest, from the target to the final focal point, was of the order of 300 ns in the laboratory frame.

At the exit of the spectrometer, two ionization chambers (MUSIC) were mounted with a niobium stripper placed in between. The MUSIC detectors delivered the energy-loss signal of fragments, thus providing the information about their atomic number. In addition, two multi-wire proportional counters were located at the exit of the FRS delivering tracking information (angle and position). Further details concerning the experimental setup can be found in Ref. [4].

The ions were identified by combining the time-of-flight, position and energy-loss information and applying the standard procedure, as described, for example, in Ref. [7].

3 Analysis of experimental data

In the experiment seven different $B\rho$ settings of the FRS were applied, which were chosen to yield optimum beam intensities of ^{231}Pa, ^{224}Pa, ^{221}Pa, ^{217}Pa, ^{214}Pa, ^{212}Pa and ^{210}Pa, respectively. The data collected in each setting were treated by using the following analysis procedure. A two-dimensional plot of the ions' position at the dispersive plane as a function of their A/q ratio was constructed. Selecting the group of events corresponding to ions which kept their charge state unchanged in both sections of the FRS, a similar two-dimensional plot showing the horizontal position at the focal plane as a function of A/q was created. This yielded a spectrum where each separated group of ions corresponded to a different isotope. After analysis of these spectra, the production cross-sections of individual isotopes were calculated according to:

$$\sigma_f = \frac{N_f}{T_{opt} T_{sec} P_0 Y} \frac{1}{N_p f_{DT} f_d}, \tag{1}$$

where N_f is the number of registered ions of a certain isotope, T_{opt} the ion-optical transmission, T_{sec} a correction for secondary reactions in the matter

placed after the target (degrader and detectors), P_0 the probability that an ion remains fully stripped in both stages of the separator, Y the correction for losses of primary beam and fragments due to nuclear reactions in the target material, N_p the total number of ^{238}U ions, f_{DT} the correction for the dead-time losses of the data acquisition system and f_d the correction for decay-losses. All production cross-sections related to nuclear reactions in the target and other matter passed by the fragments in the FRS have been calculated using the Benesh-Cook-Vary formula [8]. For these calculations it was assumed that the reaction occurs in the geometrical middle of the target, i.e. the reaction products pass through a layer of matter corresponding to the half thickness of the target.

The values of the ion-optical transmission T_{opt} have been calculated by using the Monte-Carlo simulation package MOCADI [9,10]. The transmission values were obtained separately for each $B\rho$ setting. However, due to the presence of very narrow slits in the FRS, the results of the simulation for the isotope having the smallest A/q value in a particular setting may not be reliable. Therefore, we refrain from giving production cross-sections for ^{210}Th, ^{217}Th and ^{214}Pa.

4 Results and discussion

4.1 Experimental production cross-sections

In the present experiment, the isotopic production cross-sections of light actinides have been explored by projectile fragmentation to a level as low as 1 nb. In particular, the steep descent of the yields of neutron-deficient protactinium and thorium isotopes towards the proton drip line has been mapped. The cross-sections obtained for the production of thorium and protactinium isotopes are shown in Figs. 1 and 2 and listed in Table 1 and 2, respectively. In these figures and tables, experimental data from previous studies [3] have been included for comparison. The latter data concern, however, the fragmentation of a 1 A GeV ^{238}U beam on a hydrogen target whereas a beryllium target was used in our work.

The yields (N_f in Eq. (1)) observed for ^{218}Th and ^{219}Pa are somewhat smaller than expected from a smooth decrease of the respective isotopic distributions (see Fig. 6 in Ref [4]). This is apparently due to the fact that the half-lives of these isotopes, 109(13) and 53(10) ns [11,12], respectively, are shorter than their time-of-flight through the separator (170 ns in the eigen-frame of the fragment). Therefore, for these nuclei a correction for decay-losses was applied, yielding uncertainty $1/f_d$ values (see Eq. 1) of 2.9(4) and 9(4) for ^{218}Th and

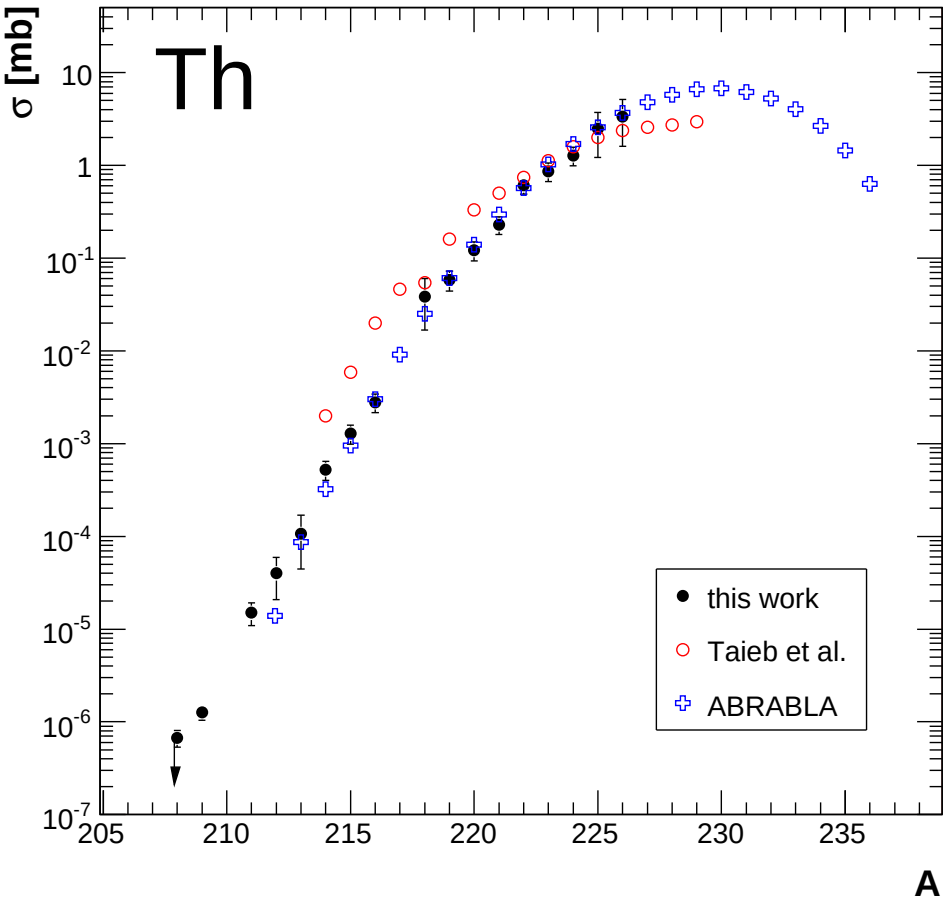

Fig. 1. Production cross-section for thorium isotopes as a function of mass number A. Full symbols mark the experimental data presented in this work. Open symbols represent the experimental results obtained by Taïeb et al. for the 1 A GeV ^{238}U fragmentation reaction on a hydrogen target [3]. Crosses show the predictions based on the abrasion-ablation model of nuclear fragmentation [13]. The data point characterised by an arrow indicates the upper limit of the production cross-section for ^{208}Th.

^{219}Pa, respectively. The corrected values of production cross-section for these isotopes are included in Figs. 1 and 2 as well as in Table 1 and 2. The σ value for ^{219}Pa, compared to the smooth descent of the distribution at its neutron-deficient side, indicates a local increase of the production cross-section. A possible explanation for this effect migth be that the ion-optical transmission simulated for this isotope may not be reliable - the A/q corresponding to the ^{219}Pa isotope was placed at the edge of the accepted A/q range for the applied $B\rho$ setting. Alternatively it may indicate that the half-life of this isotope is longer then the value given in Ref. [12].

As can be seen in Figs. 1 and 2, especially for the thorium case, reactions on

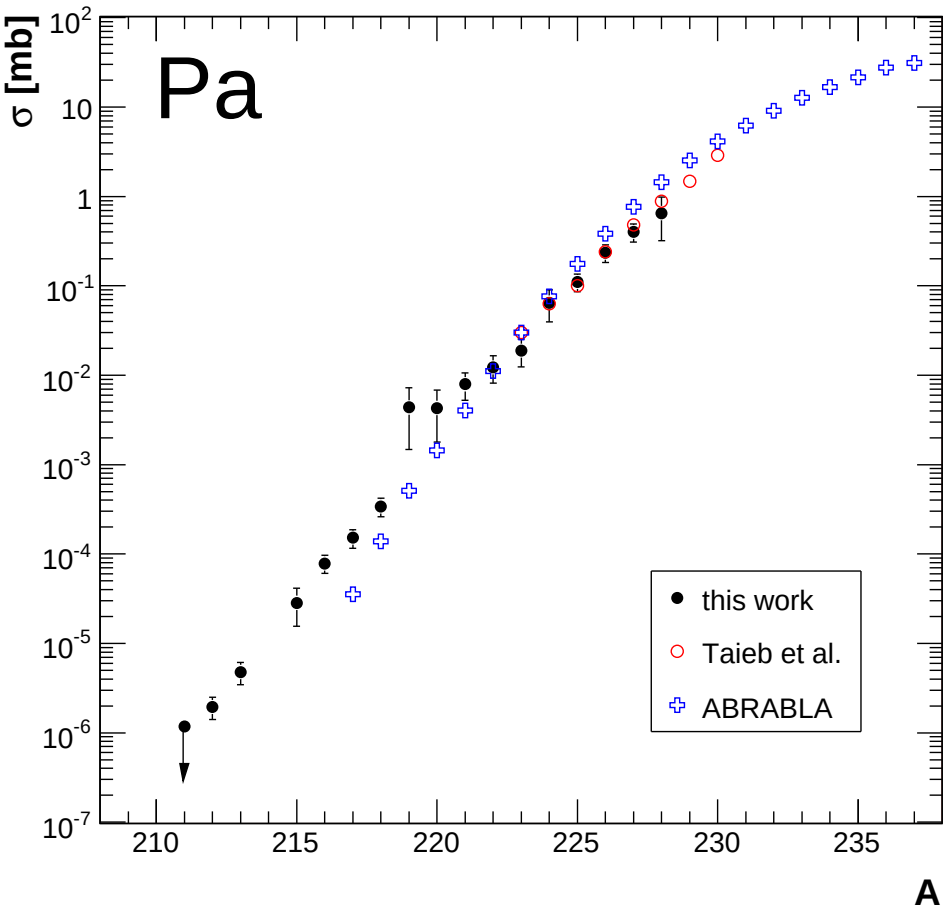

Fig. 2. Production cross-section for protactinium isotopes as a function of mass number A. Full symbols mark the experimental data presented in this work. Open symbols represent the experimental results obtained by Taïeb et al. for the 1 A GeV ^{238}U fragmentation reaction on a hydrogen target [3]. Crosses show the predictions based on the abrasion-ablation model of nuclear fragmentation [13]. The data point characterised by an arrow indicates the upper limit of the production cross-section for ^{211}Pa.

a hydrogen target yield higher production cross-sections for neutron-deficient isotopes of elements close to the projectile than the reactions on a beryllium target. This confirms the findings of previous study. It was observed that the 1 GeV proton-induced spallation of ^{208}Pb is characterised by a slightly higher cross-section for the production of neutron-deficient isotopes of the heaviest elements than the ^{208}Pb (1 A GeV)+d reaction [14]. This indicates that collisions with protons induce higher excitation energies for a given number of protons removed from the lead projectile than collisions with deuterons do. The reason for such a phenomenon may be that the collisions are more central in the former and rather peripheral in the latter case. The situation may, however, be more complex due to the high fissility of neutron-deficient pro-

tactinium and thorium isotopes.

4.2 Search for ^{208}Th and ^{211}Pa

So far the lightest known thorium and protactinium istopes are ^{209}Th [15] and ^{212}Pa [16]. In both cases the activities were produced in heavy-ion induced fusion-evaporation reactions, separated with the JAERI recoil mass separator and identified by time- and position-correlated alpha-decay chains. The production cross-sections were of the order of a 1 nb. The half-lives of ^{209}Th and ^{212}Pa were determined to be $3.8^{+6.9}_{-1.5}$ ms and $5.1^{+6.1}_{-1.9}$ ms, respectively.

We inspected our data in an attempt to find evidence for thorium and protactinium isotopes with mass number below 209 and 212, respectively. In Figs. 3 and 4 the relevant A/q distributions are shown as obtained at the final focal plane for the setting optimised for ^{212}Pa. There are indications for the occurrence of a few events at the positions corresponding to ^{208}Th and ^{211}Pa. However, the statistics and the resolution of the ion identification procedure at this setting were not sufficient to claim unambiguous observation of these isotopes. Thus, only upper limits for the corresponding production cross-section can be given as indicated in Figs. 1 and 2.

4.3 Model calculations

4.3.1 ^{238}U+Be reaction

Several years ago, the production cross-sections of neutron-deficient light actinides by fusion-fission reactions were the subject of systematic experimental studies (e.g. Ref. [17]). These experiments have shown that fission is a strongly competing decay branch in the statistical decay process and that it is essentially responsible for the decrease of the evaporation residue cross-sections as the proton drip line is approached for elements above lead. More recently, the most abundantly produced fragmentation-evaporation residues with cross-sections above 10 μb have been measured in the reaction ^{238}U+Cu at 1 A GeV [18]. Guided by these experimental results and complemented by several theoretical studies, the abrasion-ablation code ABRABLA has been developed. In the following section, we give a short outline of the ingredients of this model.

The ABRABLA code treats the projectile-fragmentation reaction in three separate stages. The first, nuclear-collision stage is formulated within the framework of the abrasion model [19,20,13] which describes the mass of the projectile-spectator as a function of the impact parameter on the basis of geometrical considerations. The N/Z ratio of the abraded nucleons is deduced

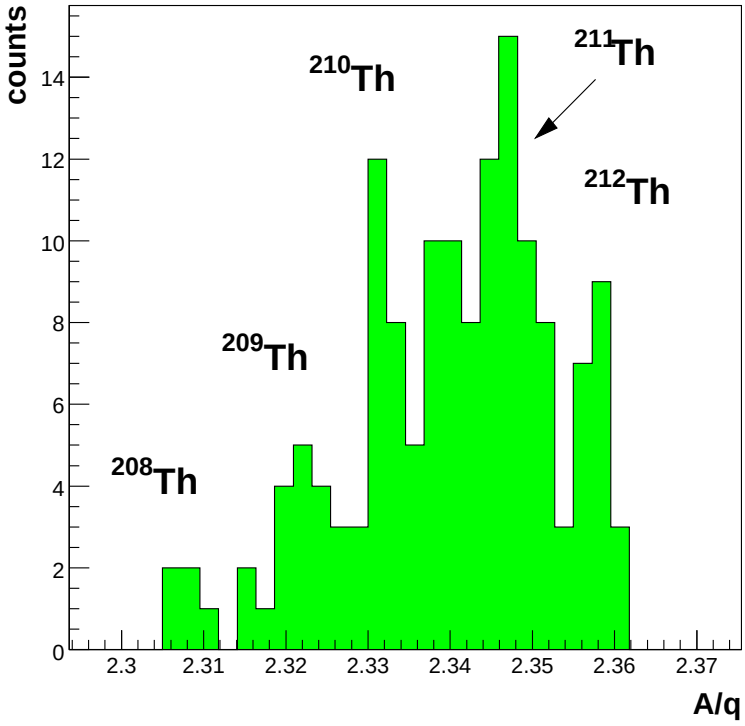

Fig. 3. Identification spectrum of thorium isotopes obtained at the final focus of the FRS for the ^{212}Pa setting.

from the hypergeometrical model [21]. The average excitation energy is deduced to be 27 MeV per abraded nucleon from isotopic distributions measured in the reaction ^{197}Au+Al [22], while the angular-momentum population is estimated on the basis of the shell model [23]. In case the excitation energy per mass of the pre-fragment exceeds a limiting value, some mass loss due to thermal instabilities of the composite system is considered [24]. In the present case, the sequential decay of the excited projectile-like remnant is treated within the statistical model following the ideas of Ref. [18] and considering the evaporation of neutrons, protons and alpha particles as well as fission as possible decay channels. In the present context, it is the formulation of the fission competition which is most decisive in determining the production cross-sections of the fragmentation residues. The competition between fission and particle evaporation is essentially governed by the number of levels above the saddle point of the compound nucleus related to the number of levels available in the daughter nuclei accessible after particle emission. As discussed in Refs. [17,18,25], it is not sufficient to consider the number of states as calculated within the framework of the independent-particle model. In particular for nuclei near the $N = 126$ shell, the different collective characters of nuclear excitations – vibrational states in the spherical ground state and predominantly rotational states at the saddle – lead to a considerable enhancement of

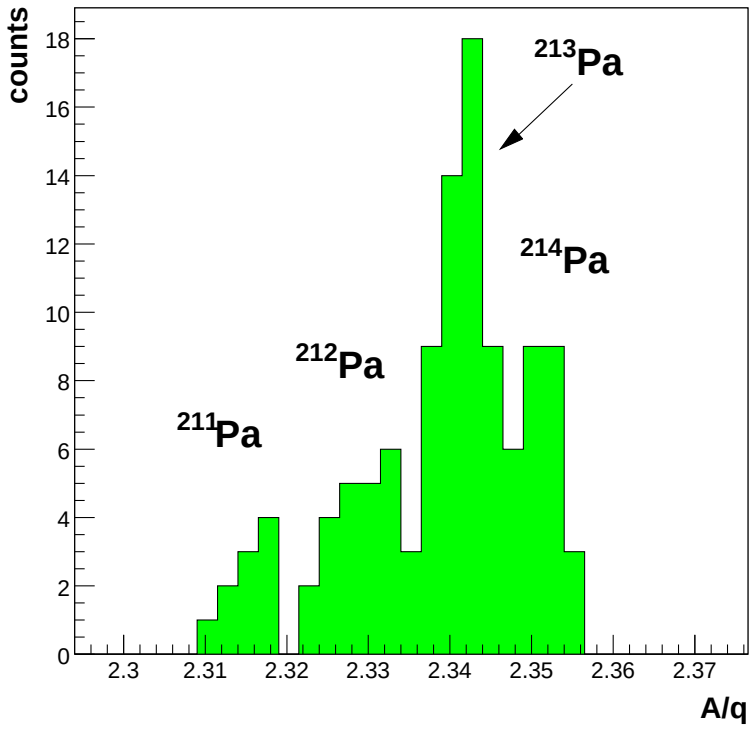

Fig. 4. Identification spectrum of protactinium isotopes obtained at the final focus of the FRS for the ^{212}Pa setting.

the fission-decay channel. From experimental observations it seems that this enhancement is just strong enough to counterbalance the stabilizing effect of the 126-neutron shell with respect to fission in the independent-particle model [17,18]. As a possible mechanism for this compensation the collective enhancement of the level density is proposed in Ref. [26]. In addition, transient effects, which suppress fission at high excitation energies, are considered following the discussion in Ref. [27].

Since ABRABLA is a Monte-Carlo code, some special precautions have to be taken to speed up the calculations with the aim of reaching very low production cross-sections. Firstly, we assumed that the influence of shell effects on the intrinsic level densities and on the collective excitations exactly cancel. Thus, binding energies, angular-momentum-dependent fission barriers and nuclear level densities were estimated on the basis of macroscopic models [28–30]. Furthermore, as discussed in Ref. [26], transient effects were considered using a simple step function for the time-dependent fission-decay width.

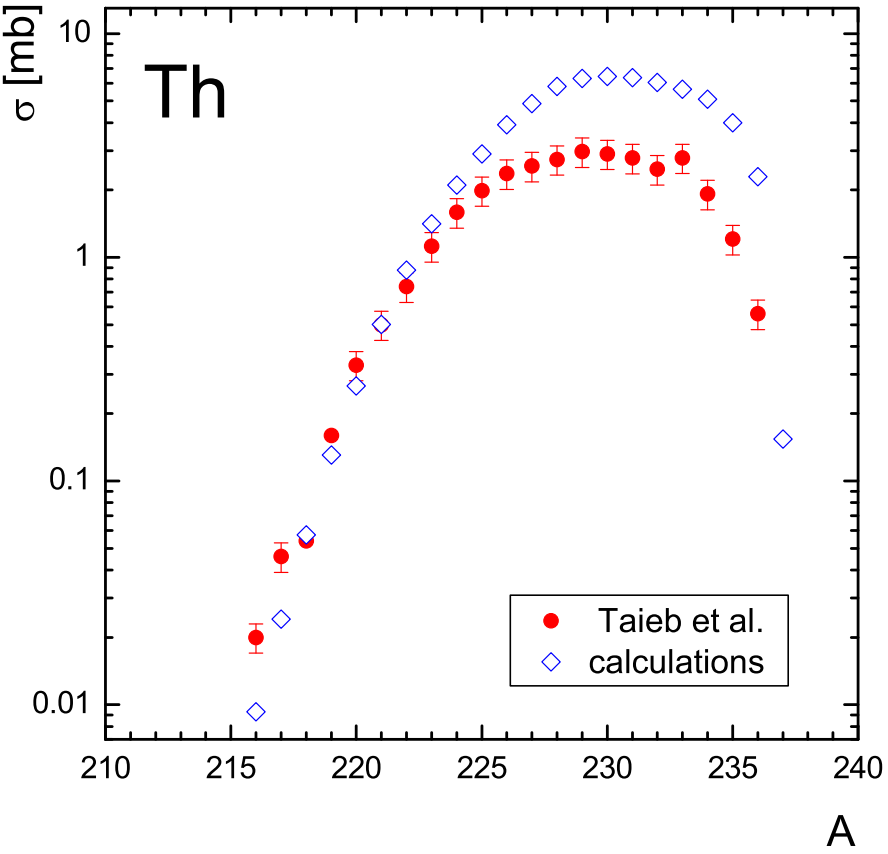

Fig. 5. Production cross-section for thorium isotopes in ^{238}U+p reaction at 1 A GeV as a function of mass number A. Full symbols represent the experimental results obtained by Taïeb et al. [3]. Diamonds show the predictions based on the intranuclear cascade model [31] coupled with ablation stage of the ABRABLA model of nuclear fragmentation [13].

4.3.2 ^{238}U+p reaction

The experimental results obtained by Taïeb et al. [3] in the ^{238}U+p reaction at 1 A GeV are compared with predictions obtained from a two-stage model calculation. Firstly, the INCL4 version of the Liège intranuclear cascade model [31] was used to calculate the excitation energy of the prefragments. Next, the ablation part of the ABRABLA model was applied for the description of the competition between evaporation of light particles (neutrons, protons, alpha particles) and fission in the deexcitation process.

4.4 Comparison of experimental and predicted production cross-section

The theoretical cross-sections for the production of thorium and protactinium isotopes in 1 A GeV ^{238}U+Be reactions, calculated with a code based on the abrasion-ablation model of nuclear fragmentation [13] including the fission

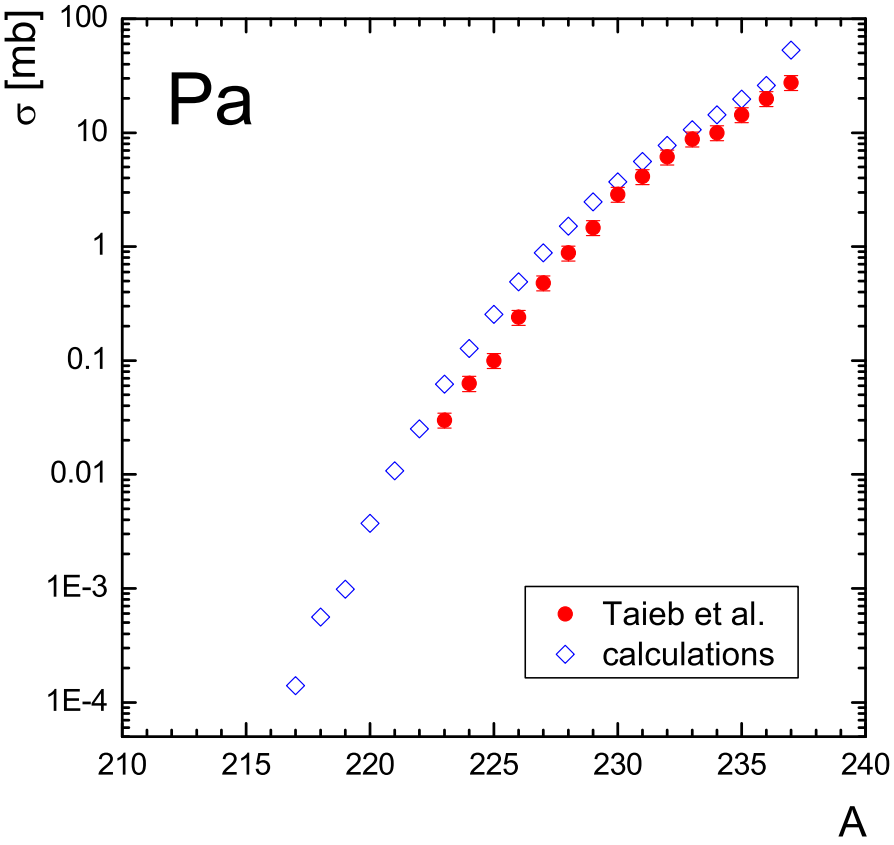

Fig. 6. Production cross-section for protactinium isotopes in ^{238}U+p reaction at 1 A GeV as a function of mass number A. Full symbols represent the experimental results obtained by Taïeb et al. [3]. Diamonds show the predictions based on the intranuclear cascade model [31] coupled with ablation stage of the ABRABLA model of nuclear fragmentation [13].

process (see sect. 4.3 for details) are displayed in Figs. 1 and 2 and listed in Tables 1 and 2. Theoretical predictions show good overall agreement with the experimental data, even though the production cross-sections are overpredicted for ^{212}Th, ^{217}Pa and ^{218}Pa and underpredicted for $^{225-228}$Pa.

We would like to stress that the results of the calculations, shown in Figures 1 and 2, were performed with the ABRABLA code as described above without any adjustment of its parameters to fit the present data. The remarkably good reproduction of the measured production cross-sections validates the physical assumptions underlying the ABRABLA code and makes it thus a valuable tool for estimating the production cross-sections of projectile-fragmentation reactions.

The cross-sections calculated for thorium and protactinium isotopes in the case of the ^{238}U+p reaction are shown in Figs. 5 and 6, respectively. The predicted production cross-section yield good overall agreement with the experimental data except for the heavy thorium isotopes, where they overestimate the mea-

sured results. The higher production cross-sections from the hydrogen target compared to the beryllium one are reproduced as well, as can be seen from a comparison of Figs. 1 and 2 with Figs. 5 and 6, respectively.

An interesting conclusion we can draw from the results presented in this work is that any enhancement of the production cross-sections connected with the considerable increase of the fission barriers of thorium and protactinium isotopes by the 126-neutron shell, i.e. for ^{216}Th and ^{217}Pa, by as much as approximately 5 MeV does not lead to any noticeable enhancement of the residue production in this region. This conclusion is not only based on the experimental results but also on the fact that they are well described by a calculation which is based on a completely macroscopic description and thus neglects any nuclear-structure effect.

5 Summary

The production cross-sections of proton-rich protactinium and thorium isotopes have been investigated by using the interaction of 1 A GeV ^{238}U ions with a beryllium target. To our knowledge, it is the first time that such cross-sections have been determined for projectile-like sub-uranium isotopes down to a level far below μb. The comparison with predictions of the abrasion-ablation model of nuclear fragmentation yields good agreement with the experimental data. A comparison with a study of the ^{238}U+p reaction shows that this reaction yields higher cross-sections for the production of fragments close to the projectile rather than the ^{238}U+d reaction investigated previously [32] or the ^{238}U+beryllium reaction described in this work.

A weak indication for the first observation of ^{208}Th and ^{211}Pa was obtained. Limited mass resolution, however, did not allow unambiguous identification of these isotopes nor the determination of their production cross-sections.

Concerning future spectroscopic studies of very neutron-deficient isotopes in this region of the nuclidic chart it would be interesting to investigate the ^{238}U+p reaction down to lower production cross-sections. Based on the data for ^{238}U+beryllium, obtained in this work, the recent upgrade of the beam intensity (10^{10} ions/spill) provided by the GSI SIS facility will yield beam intensities of isotopes such as ^{208,209}Th and ^{211}Pa that are estimated to be of the order of several hundreds per day [4]. This would allow one to perform alpha-decay measurements and to search for competing proton emission process for odd-Z nuclei. The fragmentation of a ^{238}U beam on a hydrogen target yields higher production cross-sections of light thorium and protactinium isotopes than the corresponding reactions on a beryllium target. For determining the production rates and the secondary-beam intensities of these isotopes, the re-

spective target densities have to be taken into account. Based on the thickness of 87 and 1023 mg/cm^2 used in the above-mentioned experiments, the conclusion is that a hydrogen target is superior to a beryllium one as long as the production cross-sections for the former are 30% higher than for the latter. This means that under these conditions ^{238}U+p reactions are more powerful for the study of light thorium and protactinium isotopes.

The remarkably good reproduction of the measured production cross-sections validates the physical assumptions of the ABRABLA code and makes it a valuable tool for estimating the production cross-sections of projectile-fragmentation reactions. It also validates the predictions of secondary-beam intensities in this region of the chart of the nuclides to be provided by the future FAIR facility [33], which were based on the ABRABLA code.

6 Acknowledgements

The authors would like to express their gratitude to K.-H. Behr, A. Brünle, K. Burkard, W. Hüller and M. Winkler for technical support during and in preparation for the experiment. Work at Argonne National Laboratory supported by the U.S. Department of Energy, Office of Nuclear Physics, under Contract W-31-109-ENG-38.

References

[1] E. Roeckl, The Euroschool Lectures on Physics with Exotic Beams, Vol. I, Vol. 651 of Lecture Notes in Physics, Springer, Berlin, Heidelberg, 2004, Ch. Decay Studies of N≃Z Nuclei, pp. 223–261.

[2] H.-G. Clerc, M. de Jong, T. Brohm, M. Dornik, A. Grewe, E. Hanelt, A. Heinz, A. Junghans, C. Röhl, S. Steinhäuser, B. Voss, C. Ziegler, K.-H. Schmidt, S. Czajkowski, H. Geissel, H. Irnich, A. Magel, G. Münzenberg, F. Nickel, A. Piechaczek, C. Scheidenberger, W. Schwab, K. Sümmerer, W. Trinder, M. Pfützner, B. Blank, A. Ignatyuk, G. Kudyaev, The influence of fission on the fragmentation of relativistic ^{208}Pb and ^{238}U projectiles in peripheral collisions, Nucl. Phys. A 590 (1995) 785.

[3] J. Taïeb, K.-H. Schmidt, L. Tassan-Got, P. Armbruster, J. Benlliure, M. Bernas, A. Boudard, E. Casarejos, S. Czajkowski, T. Enqvist, R. Legrain, S. Leray, B. Mustapha, M. Pravikoff, F. Rejmund, C. Stephan, C. Volant, W. Wlazło, Evaporation residues produced in the spallation reaction ^{238}U + p at 1 A GeV, Nucl. Phys. A 724 (2003) 413.

[4] Z. Liu, J. Kurcewicz, P. Woods, C. Mazzocchi, K.-H. Schmidt, F. Attallah, E. Badura, C. Davids, T. Davinson, J. Döring, H. Geissel, M. Górska, R. Grzywacz, M. Hellström, Z. Janas, M. Karny, A. Korgul, I. Mukha, M. Pfützner, C. Plettner, A. Robinson, E. Roeckl, K. Rykaczewski, K. Schmidt, D. Seweryniak, H. Weick, Decay spectroscopy of suburanium isotopes following projectile fragmentation of ^{238}U at 1 GeV/u, Nucl. Instrum. Methods Phys. Res. A 543 (2005) 591.

[5] H. Geissel, P. Armbruster, K. Behr, A. Brünle, K. Burkard, M. Chen, H. Folger, B. Franczak, H. Keller, O. Klepper, B. Langenbeck, F. Nickel, E. Pfeng, M. Pfützner, E. Roeckl, K. Rykaczewski, I. Schall, D. Schardt, C. Scheidenberger, K.-H. Schmidt, A. Schröter, T. Schwab, K. Sümmerer, M. Weber, G.Münzenberg, T. Brohm, H.-G.Clerc, M. Fauerbach, J.-J. Gaimard, A. Grawe, E. Hanelt, B. Knödler, M. Steiner, B. Voss, J. Weckenmann, C. Ziegler, A. Magel, H. Wollnik, J. Dufour, Y. Fujita, D.J.Vieira, B. Sherrill, The GSI projectile fragment (FRS): a versatile magnetic system for relativistic heavy ions, Nucl. Instrum. Methods Phys. Res. B 70 (1992) 286.

[6] B. Jurado, K.-H. Schmidt, K.-H. Behr, Application of a secondary-electron transmission monitor for high-precision intensity measurements of relativistic heavy-ion beams, Nucl. Instrum. Methods Phys. Res. A 483 (2002) 603.

[7] M. Pfützner, P. Regan, P. Walker, M. Caamaño, J. Gerl, M. Hellström, P. Mayet, K.-H. Schmidt, Z. Podolyák, M. Mineva, A. Aprahamian, J. Benlliure, A. M. Bruce, P. A. Butler, D. C. Gil, D. M. Cullen, J. Döring, T. Enquist, C. Fox, J. G. Narro, H. Geissel, W. Gelletly, J. Giovinazzo, M. Górska, H. Grawe, R. Grzywacz, A. Kleinböhl, W. Korten, M. Lewitowicz, R. Lucas, H. Mach, C. D. O'Leary, F. D. Oliveira, C. J. Pearson, F. Rejmund, M. Rejmund, M. Sawicka, H. Schaffner, C. Schlegel, K. Schmidt, C. Theisen, F. Vivès, D. D. Warner, C. Wheldon, H. J. Wollersheim, , S. Wooding, Angular momentum population in the fragmentation of ^{208}Pb at 1 GeV/nucleon, Phys. Rev. C 65 (2002) 064604.

[8] C. Benesh, B. Cook, J. Vary, Single nucleon removal in relativistic nuclear collisions, Phys. Rev. C 40 (1989) 1198.

[9] N. Iwasa, H. Geissel, G. Münzenberg, C. Scheidenberger, T. Schwab, H. Wollnik, Mocadi, a universal monte carlo code for the transport of heavy ions through matter within ion-optical systems, Nucl. Instrum. Methods Phys. Res. B 126 (1997) 284.

[10] http://www-linux.gsi.de/˜weick/mocadi.

[11] Y. A. Akovali, Nuclear Data Sheets Update for A=218, Nuclear Data Sheets 76 (1995) 457.

[12] E. Browne, Nuclear data sheets for A=215,219,223,227-, Nucl. Data Sheets 65 (1992) 669.

[13] J.-J. Gaimard, K.-H. Schmidt, A reexamination of the abrasion-ablation model for the descrption of the nuclear fragmentation reaction, Nucl. Phys. A 531 (1991) 709.

[14] T. Enqvist, P. Armbruster, J. Benlliure, M. Bernas, A. Boudard, S. Czajkowski, R. Legrain, S. Leray, B. Mustapha, M. Pravikoff, F. Rejmund, K.-H. Schmidt, C. Stéphan, J. Taieb, L. Tassan-Got, F. Vivès, C. Volant, W. Wlazło, Primary-residue production cross sections and kinetic energies in 1 A GeV ^{208}Pb on deuteron reactions, Nucl. Phys. A 703 (2002) 435.

[15] H. Ikezoe, T. Ikuta, S. Hamada, Y. Nagame, I. Nishikana, K. Tsukada, Y. Oura, T.Ohtsuki, α decay of new isotope ^{209}Th, Phys. Rev. C 54 (1996) 2043.

[16] S. Mitsuoka, H. Ikezoe, T. Ikuta, Y. Nagame, K. Tsukada, I. Nishinaka, Y. Oura, Y. Zhao, α decay properties of the new neutron deficient isotope ^{212}Pa, Phys. Rev. C 55 (1997) 1555.

[17] K.-H. Schmidt, W. Morawek, The conditions for the synthesis of heavy nuclei, Rep. Prog. Phys. 54 (1991) 949.

[18] A. R. Junghans, M. de Jong, H.-G. Clerc, A. V. Ignatyuk, G. A. Kudyaev, K.-H. Schmidt, Projectile-fragment yields as a probe for the collective enhancement in the nuclear level density, Nucl. Phys. A 629 (1998) 635.

[19] J. D. Bowman, W. J. Swiatecki, C. E. Tsang, Abrasion and Ablation of Heavy Ions, UNCLAS Reprint LBL-2908.

[20] L. F. Oliveira, R. Donangelo, J. O. Rasmussen, Abrasion-ablation calculations of large fragment yields from relativistic heavy ion reactions, Phys. Rev. C 19 (1979) 826.

[21] J. Hüfner, K. Schäfer, B. Schürmann, Abrasion-ablation in reactions between relativistic heavy ions, Phys. Rev. C 12 (1975) 1888.

[22] K.-H. Schmidt, T. Brohm, H.-G. Clerc, M. Dornik, M. Fauerbach, H. Geissel, A. Grewe, E. Hanelt, A. Junghans, A. Magel, W. Morawek, G. Münzenberg, F. Nickel, M. Pfützner, C. Scheidenberger, K. Sümmerer, D. Vieira, B. Voss, C. Ziegler, Distribution of Ir and Pt isotopes produced as fragments of 1 A GeV 197Au projectiles: a thermometer for peripheral nuclear collisions, Phys. Lett. B 300 (1993) 313.

[23] M. de Jong, A. V. Ignatyuk, K. H. Schmidt, Angular momentum in peripheral fragmentation reactions, Nucl. Phys. A 613 (1997) 435.

[24] K.-H. Schmidt, M. V. Ricciardi, S. Botvina, T. Enqvist, Production of neutron-rich heavy residues and the freeze-out temperature in the fragmentation of relativistic ^{238}U projectiles determined by the isospin thermometer, Nucl. Phys. A 710 (2002) 157.

[25] A. V. Ignatyuk, K. K. Istekov, G. N. Smirenkin, The influence of collective effects on the competition of fission and neutron emission in the vicinity of the N=126 shell, Yad. Fiz. 37 (1983) 831, sov. J. Nucl. Phys. 37 (1983) 495.

[26] K.-H. Schmidt, J. G. Keller, D. Vermeulen, Temperature-induced deformation - a possible mechanism for washig out spherical effects in the nuclear level density, Z. Phys. A 315 (1984) 159.

[27] B. Jurado, C. Schmitt, K.-H. Schmidt, J. Benlliure, A. Junghans, A critical analysis of the modelling of dissipation in fission, Nucl. Phys. A 747 (2005) 14.

[28] P. Möller, J. R. Nix, W. D. Myers, W. J. Swiatecki, Nuclear ground-state masses and deformations,, At. Data Nucl. Data Tables 59 (1995) 185.

[29] A. J. Sierk, Macroscopic model of rotating nuclei, Phys. Rev. C 33 (1986) 2039.

[30] A. V. Ignatyuk, M. G. Itkis, V. N. Okolovich, G. N. Smirenkin, A. S. Tishin, Fission of pre-actinide nuclei. excitation functions of the (α, f) reaction, Yad. Fiz. 21 (1975) 1185, (Sov. J. Nucl. Phys. 21 (1975) 612).

[31] A. Boudard, J. Cugnon, S. Leray, C. Volant, Intranuclear cascade model for comprehensive description of spallation reaction data, Phys. Rev. C 66 (2002) 044615.

[32] E. Casarejos, P. Armbruster, L. Audouin, J. Benlliure, M. Bernas, A. Boudard, R. Legrain, S. Leray, B. Mustapha, S. Czajkowski, T. Enqvist, B. Fernandez, J. Pereira, M. Pravikoff, F. Rejmund, K.-H. Schmidt, C. Stephan, J. Taieb, L. Tassan-Got, C. Villagrasa, C. Volant, W. Wlazlo, Isotopic Production Cross Sections of Residues in Reactions Induced by Relativistic Heavy Ions with Protons and Deuterons, Phys. At. Nucl. 66 (2003) 1413.

[33] Fair design report, http://www.gsi.de/fair.

Table 1: Numerical values of the production cross-sections for thorium isotopes. The results from this work (σ_1) on the 1 A GeV ^{238}U+Be reaction are given together with their uncertainties ($\delta\sigma_1$) and compared to the corresponding experimental data (σ_2, $\delta\sigma_2$) obtained by Taïeb et al. [3] for the 1 A GeV ^{238}U+p reaction and to Monte-Carlo predictions (σ_{theor}) based on the abrasion-ablation model [13] for the 1 A GeV ^{238}U+Be reaction.

Z	A	$\sigma_1(\delta\sigma_1)$ [mb]	$\sigma_2(\delta\sigma_2)$ [mb]	σ_{theor} [mb]
90	208	$< 6.7(14) \cdot 10^{-7}$		
90	209	$1.3(2) \cdot 10^{-6}$		
90	210	–		
90	211	$1.6(4) \cdot 10^{-5}$		
90	212	$4.5(19) \cdot 10^{-5}$		$1.38 \cdot 10^{-5}$
90	213	$1.4(6) \cdot 10^{-4}$		$8.63 \cdot 10^{-5}$
90	214	$5.2(12) \cdot 10^{-4}$	$2.0(3) \cdot 10^{-3}$	$3.21 \cdot 10^{-4}$
90	215	$1.3(3) \cdot 10^{-3}$	$5.9(9) \cdot 10^{-3}$	$9.52 \cdot 10^{-4}$
90	216	$2.8(6) \cdot 10^{-3}$	0.020(3)	0.00301
90	217	–	0.046(7)	0.00911
90	218	$3.9(22) \cdot 10^{-2}$	0.054(8)	0.0250
90	219	$5.8(14) \cdot 10^{-2}$	0.16(2)	0.0608
90	220	0.12(3)	0.33(5)	0.139
90	221	0.23(5)	0.50(8)	0.294
90	222	0.61(11)	0.7	0.570
90	223	0.86(19)	1.1(2)	1.02
90	224	1.3(3)	1.6(2)	1.69
90	225	2.5(13)	2.0(3)	2.59
90	226	3.4(18)	2.4(4)	3.66
90	227		2.6(4)	4.77
90	228		2.7(4)	5.79

90	229	3.0(4)	6.66
90	230	2.9(4)	6.75
90	231	2.8(4)	6.16
90	232	2.5(4)	5.24
90	233		4.03
90	234	1.9(3)	2.67
90	235		1.45
90	236	0.6(1)	0.63

Table 2: Numerical values of the production cross-sections for protactinium isotopes. The results from this work (σ_1) on the 1 A GeV ^{238}U+Be reaction are given together with their uncertainties ($\delta\sigma_1$) and compared to the corresponding experimental data (σ_2, $\delta\sigma_2$) obtained by Taïeb et al. [3] for the 1 A GeV ^{238}U+p reaction and to Monte-Carlo predictions (σ_{theor}) based on the abrasion-ablation model [13] for the 1 A GeV ^{238}U+Be reaction.

Z	A	$\sigma_1(\delta\sigma_1)$ [mb]	$\sigma_2(\delta\sigma_2)$ [mb]	σ_{theor} [mb]
91	211	$< 1.2(2) \cdot 10^{-6}$		
91	212	$1.9(5) \cdot 10^{-6}$		
91	213	$4.7(13) \cdot 10^{-6}$		
91	214	–		
91	215	$2.5(13) \cdot 10^{-5}$		
91	216	$7.7(18) \cdot 10^{-5}$		
91	217	$1.5(4) \cdot 10^{-4}$		$3.4 \cdot 10^{-5}$
91	218	$3.4(8) \cdot 10^{-4}$		$1.4 \cdot 10^{-4}$
91	219	$4.4(29) \cdot 10^{-3}$		$5.1 \cdot 10^{-4}$
91	220	0.0043(25)		0.0014
91	221	0.008(3)		0.0040
91	222	0.012(4)		0.011
91	223	0.019(6)	0.030(5)	0.030
91	224	0.06(3)	0.063(9)	0.076
91	225	0.11(3)	0.100(15)	0.18
91	226	0.23(5)	0.24(4)	0.38
91	227	0.40(9)	0.48(7)	0.77
91	228	0.7(3)	0.88(13)	1.4
91	229	9(5)	1.47(22)	2.5
91	230		2.9(4)	4.1
91	231		4.1(6)	6.2

91	232	6.1(9)	9.1
91	233	8.8(13)	12.6
91	234	10.0(15)	16.6
91	235	20(3)	21.5
91	236	27(4)	27.6
91	237		31.2